Light Metals 2015
Edited by: Margaret Hyland
TMS (The Minerals, Metals & Materials Society), 2015

CHARACTERIZING AND MODELING THE DEFORMATION OF AA5182 FOR HOT BLANK – COLD DIE (HB-CD) STAMPING

Nan Zhang[1], Fadi Abu-Farha[1]
[1]Automotive Engineering, Clemson University; 4 Research Drive; Greenville, SC, 29607, USA

Keywords: Hot Blank – Cold Die Stamping, Aluminium Sheet, Modeling, Digital Image Correlation, Deformation Mechanisms

Abstract

Though warm and hot sheet forming operations enhance the limited formability of aluminium alloys, the high cost and low production rates make them unfit for the demanding automotive sector. A non-isothermal stamping approach, referred to as hot blank - cold die (HB-CD), promises a fast/economic alternative while overcoming the limited formability issues of the material. This, however, necessitates characterizing and modeling the complex material behavior over a wide range of temperatures and strain rates, which is the prime focus of this work. Detailed mechanical testing, aided by digital image correlation (DIC), is carried out on an automotive-grade 5182 aluminium alloy sheet. A phenomenological model is developed and is shown to successfully capture the isothermal behavior of the material over the full temperature/strain rate range for HB-CD stamping.

Introduction

Aluminum–magnesium alloys (AA5xxx) have high strength-to-weight ratios that make them good candidates for replacing conventional steels in automotive body panels. At ambient temperatures, AA5xxx sheets exhibit limited formability that does not permit forming complex parts. In addition, serrated yielding and the Portevin-Le Chartelier (PLC) effect, observed between room temperature and 100 ºC [1-3], adversely affect the surface quality of the material and thus exclude it from application in outer body panels. To overcome these issues, hot forming at elevated temperatures (>300 ºC) and low speeds (<0.01 s^{-1}) have been attempted. Superplastic forming (SPF) and quick plastic forming (QPF) gained significant interest, and even automotive use, with several 5xxx alloys [4]. The extreme tensile ductility (>200%) enabled forming complex parts that could not be formed by conventional techniques. Flow behavior, formability and deformation mechanisms have been investigated for several AA5xxx sheets at a wide range of SPF/QPS conditions [5-8]. However, the high material cost (fine-grained material), the very high energy cost and low production volumes have ever put a major constraint on their use on a large scale.

Although their formability in the warm temperature range (~150 to ~300 ºC) is not as good as hot forming, AA5xxx sheets still exhibit significant improvement in formability compared to that at ambient temperatures. Evidence to this can be seen in AA5182-O; one of the most popular automotive grade Al-Mg sheet materials [9-11]. In spite of this, warm sheet forming operations have not gained an appreciable level of application in the automotive sector. The fact that the setup is heated in warm forming implies considerable amounts of energy (even though the temperatures are lower than SPF/QPF) and limitation to the forming speeds, both of which are challenging to fit an automotive environment.

An alternative process, referred to as hot blank – cold die (HB-CD) stamping, is proposed as a compromise between cold and warm/hot forming processes, to advance the use of lightweight sheet materials, such as AA5xxx sheets. A schematic of the process is shown in Figure 1. In it, the blank is heated to a selected temperature and then transferred to a cold die/press to be stamped into a particular geometry. Heating the blank provides the boost in ductility needed to deform the material and form the part; heating only the blank implies much lower energy needs compared to any form of warm/hot forming. Additionally, stamping in cold dies means a fit to the current stamping infrastructure, and the ability to achieve similar production volumes. HB-CD stamping is simply equivalent to "hot stamping of boron steels"; the approach is similar, yet the temperatures are much lower, there is no quenching component, and there is no phase transformation. Hot stamping of boron steels is a widely used process; almost every car produced today has a hot-stamped component. HB-CD has thus great potentials for forming hard-to-deform non-ferrous materials (aluminium and magnesium) into cost-effective high-volume automotive components.

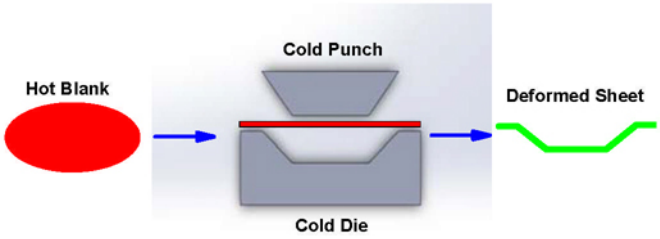

Figure 1: schematic of the HB-CD stamping process.

Though the process is simple, the non-isothermal nature of material deformation during HB-CD is complex. This requires examination of material behavior over a wide range of conditions, mainly temperatures spanning between the initial temperature of the blank and room temperature. Moreover, for finite element simulations of the process, a constitutive model that can capture the isothermal flow behavior of the material over the entire temperature range is needed. This work will address these two items, wide ranging material characterization and constitutive modeling, for a selected AA5182 sheet.

Experiments

Material

For the present investigation, a 2.0mm thick 5182 aluminium alloy sheet, received in the annealed condition, was used. The material's chemical composition is provided in Table 1. The initial microstructure of the as-received material was examined using a Zeiss AxioVert A1 inverted microscope. Specimens were polished and then electrochemically etched using Baker's Etch. An example of the grain structure in the RD-ND plane, revealed under polarization at 200x, is shown in Figure 2. The average grain size was measured to be 18.38±5µm by averaging the results from over 30 measurements (vertical, horizontal and diagonal lines) in different regions.

Element	Al	Mg	Mn	Fe	Si
wt%	Balance	4.53	0.24	0.07	0.05

Table 1: Chemical composition (wt%) of the AA5182-O sheet used in this work

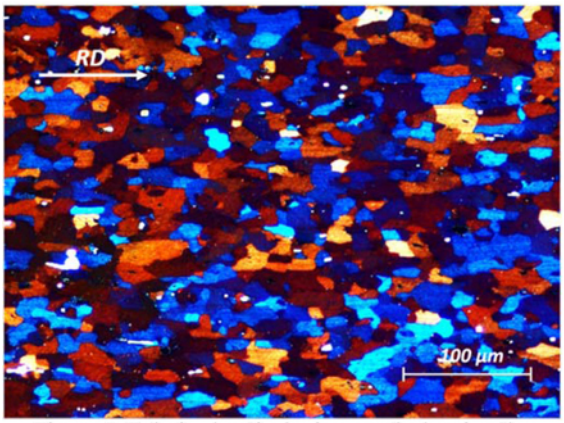

Figure 2: Polarized optical micrograph showing the microstructure of the as-received material.

Setup

A uniaxial tensile testing machine, INSTRON 5985, fitted with a convection furnace, was used here, as shown in Figure 3a. Since a wide range of temperatures is covered in this work, the specimen geometry and grip design were made following a previous effort on uniaxial tensile testing of metallic superplastic sheets [12]. The as-received AA5182-O sheets were waterjet-cut into specimens according to the particular geometry shown in Figure 3b. The gauge region has 8mm width and 30mm shoulder-shoulder length; small 3mm-radius fillets were applied to the ends, leaving a parallel-side length of 24mm. The custom-made quick-mount grips were designed to enable fast loading of test specimens (minimize heating time), as well as pulling on the shoulder area (to minimize material flow into the gage region).
As the state-of-the-art non-contact strain measurement technique, digital image correlation (DIC) reveals high levels of details about material deformation that cannot be matched by any of the predecessor techniques. Commercial DIC systems have gained wide use for material property characterization in the recent decade. A DIC system, ARAMIS 5M, has thus been used in this work to closely examine the deformation of the material over the entire gage region. The system was also used to eliminate the compliance of the setup (load frame, grips and connectors), and produce accurate stress/strain curves, especially at higher temperatures. To enable DIC strain measurements, test specimens were lightly polished (emery paper equivalent of 320 grit size or finer), cleaned, then speckle-patterned with high-temperature black and white paint, as demonstrated in Figure 3a.

Tensile Tests

For HB-CD of AA5182, the initial temperature of the blank is not expected to exceed 350 ºC. Therefore, tensile tests were carried out at 25ºC, 100ºC, 150ºC, 200ºC, 250ºC and 300 ºC, covering five true strain rates per temperature: 0.001, 0.003, 0.01, 0.03 and 0.1 s^{-1}. Before testing, the entire setup is first heated to the desired temperature and allowed to equilibrate for at least 2 hours. To start, a specimen is quickly loaded into the grips; the chamber is closed and allowed to equilibrate again for ~3 minutes. Meanwhile, a small pre-load (~15N) is applied to guarantee initial contact between specimen shoulders and grips. A test is then run while capturing images with the DIC system at a sufficient rate (~250 to 500 image pairs per test) until failure. Tests were repeated at least twice per temperature and strain rate combination to ensure reliability of generated data. All the specimens tested in this work were cut along the sheet's rolling direction.

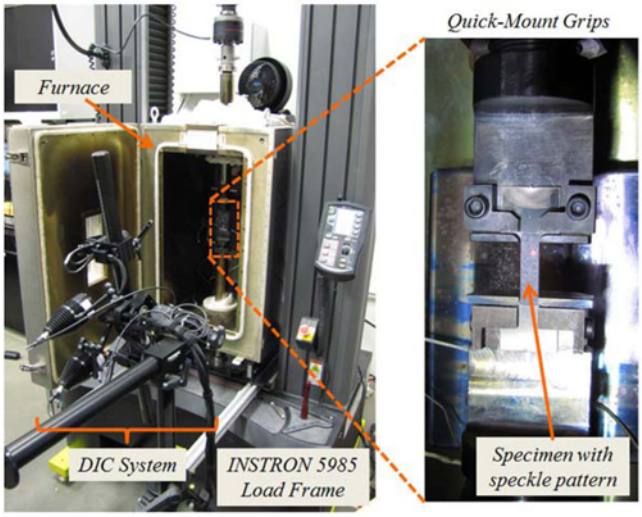

(a)

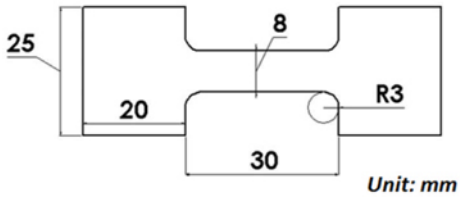

(b)

Figure 3: (a) experimental setup for tensile testing at higher-than-ambient temperatures, featuring a universal tensile tester, a furnace and a DIC system, (b) test specimen geometry.

Experimental Results

Portevin-Le Chatelier (PLC) Effect

The phenomenon and mechanism of PLC effect has been well-studied and documented in the literature [13-15]. Type-A PLC effect was observed in the material at lower temperatures with the aid of DIC. Considering Type A PLC band is periodically initiated and propagated within the gage area, we focus here on one cycle of a band movement. The propagation of a PLC band in a test specimen deforming at 25 ºC and 0.01 s^{-1}, is shown in Figure 4. From a strain rate perspective, part (a), the PLC band is initiated at one end of the gage region at ~45° relative to the tensile direction. The strain rate within the band width is much higher than the rest of the specimen. From the subsequent images after band initiation, it is seen that the band propagates to the other end of gage area at a constant speed; after that the band weakens and ultimately disappears until the next propagation. According to the strain field evolution, shown in part (b) of the figure, the deformation before and after the band is considerably uniform. As soon as the band is formed, strain grows by a small amount in the field where PLC band sweeps over.

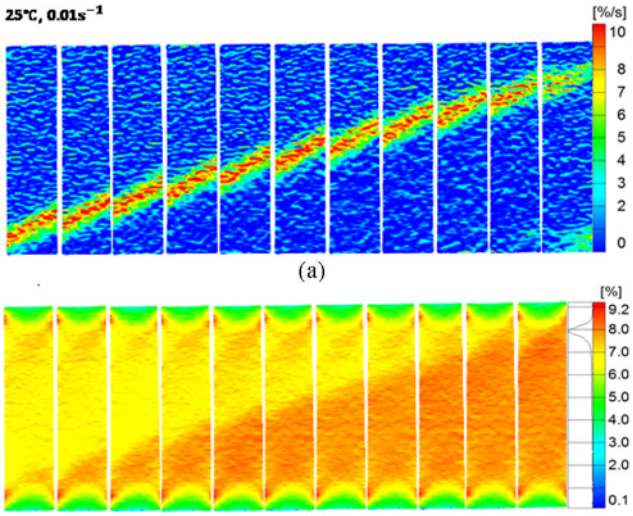

Figure 4: Propagation cycle of a PLC band in the material (shown here at 25 ºC and 0.01 s^{-1}) noted through (b) strain rate and (b) strain field evolutions.

Stress/Strain Curves

All the stress-strain curves presented in this paper were extracted from the DIC analysis results. The true stress/strain curves for the lower temperatures, 25 and 100 ºC are shown in Figure 5. Serration yielding, agreeing with earlier observations from DIC strain maps, is clearly observed in both cases. The critical strain for serration yielding is not of a prime focus in this work; nonetheless, it is noted that the onset of serration yielding is postponed by increasing the temperature. The identification of PLC type at different experimental conditions is not a concern here; it will be investigated in a different work. The stress/strain curves for both temperatures are almost identical, showing no effect of temperature on the overall hardening behavior. Also, though not significant, higher strain rates produce relatively lower flow stresses, implying negative strain rate sensitivity (SRS). This unique stress-strain behavior, including serration yielding, is associated with dynamic strain aging (DSA) in the material [16, 17], and has been explained as a macroscopic result of interactions between solute substitutional atoms (such as magnesium in this case) and dislocations [3, 18].

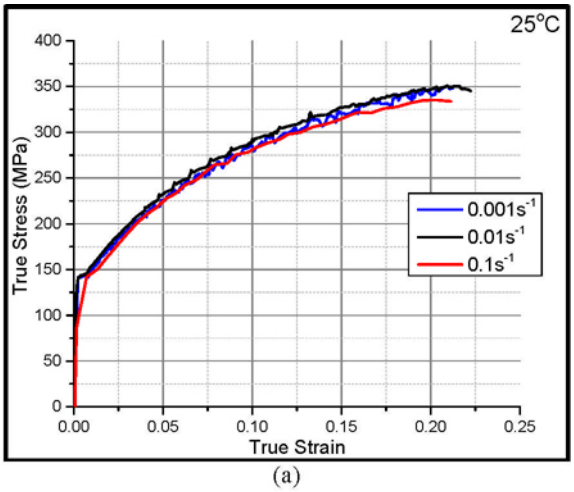

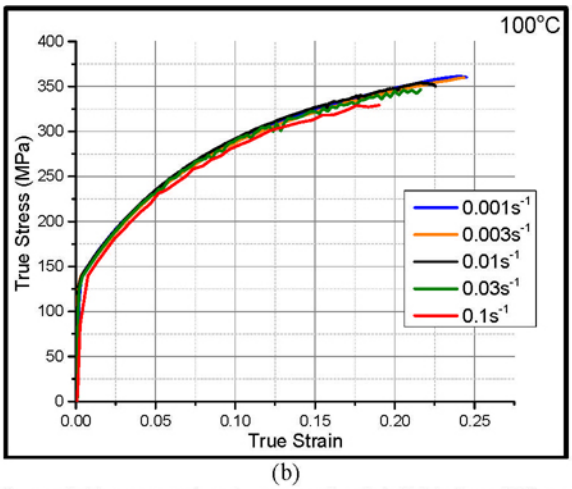

Figure 5: True stress/strain curves for AA5182-O at different strain rates, for a selected temperature of (a) 25 ºC, (b) 100 ºC.

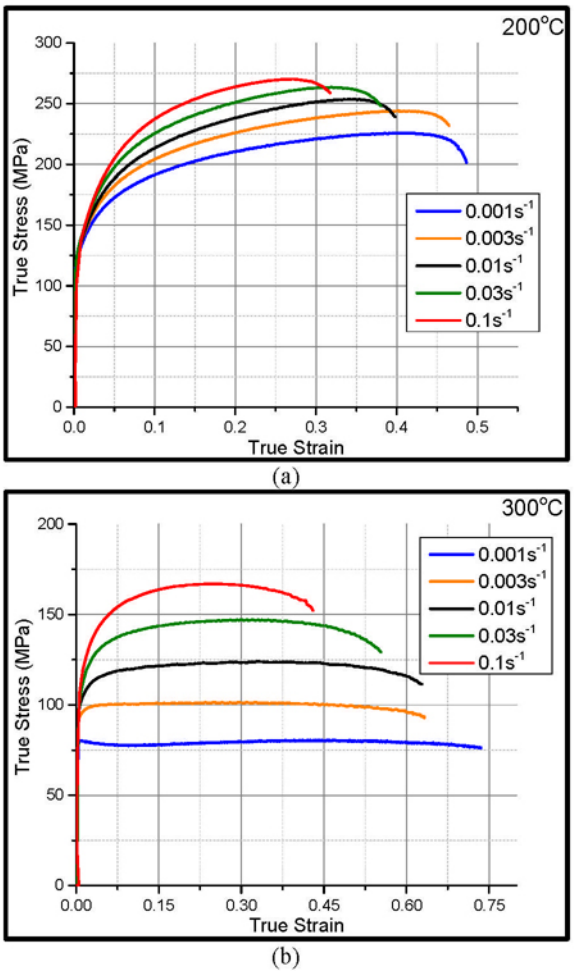

Figure 6: True stress/strain curves for AA5182-O at different strain rates, for a selected temperature of (a) 200 ºC, (b) 300 ºC.

With the increase in temperature, PLC effect and serration yielding completely disappear at and above 150 ºC, while SRS gradually moves out of the negative region. At 200 ºC, the true stress/strain curves are shown in Figure 6a; lower strain rates globally lead to lower flow stress levels, which means the

corresponding SRS has turned positive [16, 17]. The response of total elongation to drop in strain rate is apparent, with material tensile ductility exceeding 60%. Strain hardening is still evident in all the stress/strain curves at this temperature. However, the softening effect becomes stronger with further temperature increase, as demonstrated by the stress/strain curves at 300 ºC, shown in Figure 6b. Near perfectly-plastic behavior is noted at low strain rates; hardening is only observed at the initial stages of deformation at higher strain rates.

Deformation Mechanisms

At elevated temperatures, the deformation of aluminum alloys generally involves creep flow and grain boundary sliding. To identify the deformation mechanisms in the different regimes of experimental conditions, the phenomenological governing equation developed by Sherby and Burke 1968 [19], and used later in multiple efforts, such as Taleff et al. [5, 20], is used here:

$$\dot{\varepsilon} = AD\left(\frac{\mathbf{b}}{d}\right)^{p}\left(\frac{\sigma}{E}\right)^{n} \quad (1)$$

where D is the appropriate diffusivity for the controlling creep mechanism, $\mathbf{b}$ is the magnitude of Burgers vector, d is grain size, p is the grain size exponent, n is the stress exponent which approximately equals the inverse of SRS, and σ is the flow stress. The Dynamic Young's modulus is dependent on temperature according to the expression [7]:

$$E = 77630 + 12.98T - 0.03084T^{2} \quad (2)$$

The stress exponent in Equation 1, n, has been utilized to indicate the distinguished deformation mechanism at various experimental conditions [5, 6, 20]. To take the effects of the various temperatures into consideration, the normalization of strain rate chosen here is the in the form of the Zener-Hollomon parameter:

$$Z = \dot{\varepsilon}\exp(\frac{Q}{RT}) \quad (3)$$

where R is the gas constant (R = 8.31J/mol-K) and T is the temperature in Kelvin. The activation energy Q was set to 142kJ/mol.K since self-diffusion of magnesium and aluminium are similar [21]. Based on the above equations, a Z-plot for the material is generated, as presented in Figure 7 below.

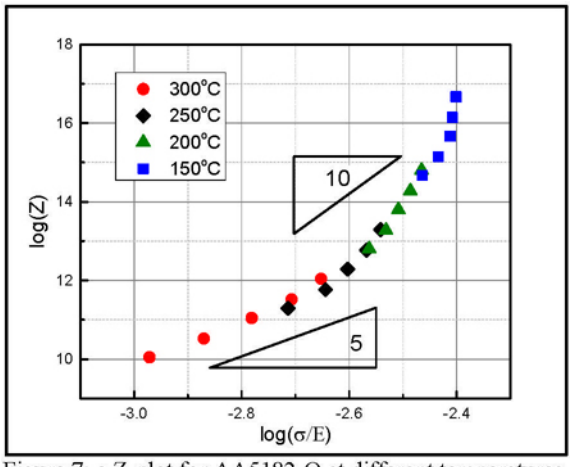

Figure 7: a Z-plot for AA5182-O at different temperatures.

In this plot, the n value is measured as the slope within a certain segment of the curve. In the lower temperatures region (<200 ºC), power-law breakdown is found to be the dominant deformation mechanism, since ($n \gg 5$). Note the sharp increase in n at 150 ºC, even when compared to 200 ºC. The spike in n continues at lower temperatures (though not shown in the plot), with significant DSA at temperatures below 100 ºC (as detailed earlier). On the other hand, as the forming temperature increases, the n value gradually decreases until it reaches approximately 5 at 300 ºC, which is a strong indicative of dislocation climb. The Z-plot clearly shows this shift in deformation mechanisms around ~250 ºC.

Constitutive Modeling

Model Development and Fitting

Phenomenological constitutive models for the deformation of aluminium alloy sheets, both at ambient and higher-then-ambient temperatures, have been extensively used, and are well documented in the literature, due to their simplicity and convenience for implementation in finite element (FE) codes. Considering that strain hardening controls plastic deformation in the temperature range from ambient to ~200 ºC, as inferred from the stress/strain curves in Figure 8, the power-law model and its modifications (such as the Holloman, Swift, Wagoner and Nadai models) have been widely-used for modeling material deformation at quasi-static rates [10, 11, 22-24]. Those power-law based models have been proven capable of describing the material hardening behavior within a limited range of experimental conditions (mainly temperature). However, for modeling HB-CD, the wider range of temperatures implies accounting for multiple deformation mechanisms (as identified earlier) that a simple model cannot capture. For AA5182-O in this case, the softening behavior plays a more imperative role at higher temperatures, and the stress/strain curves no longer obey the power-law, as evident from Figure 8 (note the large strains and shift towards perfectly-plastic behavior). Therefore, to extend such models to fit the stress/strain curves to wider temperature ranges, thermal softening and accommodating large strains become two inevitable factors.

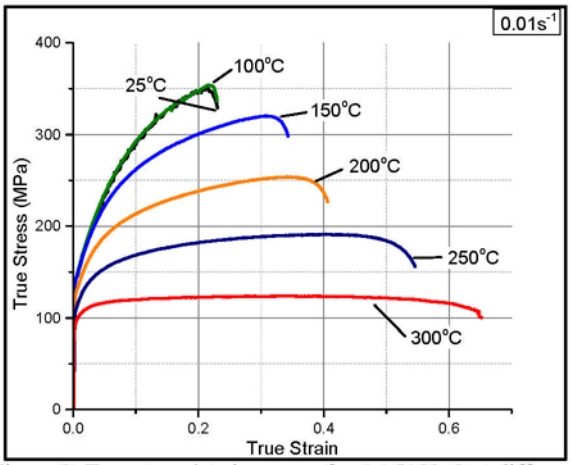

Figure 8: True stress/strain curves for AA5182-O at different temperatures, for a selected strain rate of 0.01 s^{-1}.

To couple the softening effect, the general approach is to introduce another temperature-dependent (typically inverse) term to the model. For instance, Cheng et al. 2008 [25] applied an

exponential term in his work to extend the power-law model to fit AZ31 (which exhibits strong softening behavior) in the temperature range from 150 to 300 ºC. Xing et al. 2009 [26] also introduced an exponential softening term to a hardening model for Boron steel (22MnB5). However, the effects of such softening terms are critical, because the softening degree varies not only with temperature, but also with strain rate and strain history. The deformation of AA5182-O at higher temperatures can be regarded as a competitive process between hardening and softening. For instance, based on the flow curves at 300 ºC (Figure 6b), hardening behavior can still be observed at higher strain rates (> 0.03 s^{-1}), while the curves at lower strain rates (<0.003 s^{-1}) are dominated by a softening behavior.

A new phenomenological model is proposed in this work for capturing the behavior of AA5182-O over the entire range of HB-CD, using a piece-wise function as follows:

$$\sigma = \begin{cases} K\varepsilon^{n}\left(\dfrac{\dot{\varepsilon}}{\dot{\varepsilon}_r}\right)^{m} & 298K \le T \le 373K \\ \sigma_{peak} - \sqrt{a\exp(b\cdot\varepsilon)} & 373K < T \le 573K \end{cases} \quad (4)$$

At low temperatures (cold forming at 25-100 ºC), the power-law model is used to describe the simple hardening behavior of the material. The parameters were extracted by fitting the experimental data in Figure 5, yielding $K = 560\ MPa$ and $n = 0.28$. The negative strain rate sensitivity, associated with dynamic strain aging (DSA), is accounted for with a constant $m = -0.007$ value. On the other hand, the second function in Equation 4 describes material behavior at higher temperatures (warm to high forming at 150-300 ºC). σ_{peak} is the peak or steady-state stress value, which is predicted by a polynomial function of the Zener-Hollomon parameter:

$$\sigma_{peak} = -0.5285\cdot[\ln(Z)]^2 + 47.808\cdot\ln(Z) - 744.47 \quad (5)$$

where a and b are two parameters, which by fitting to the experimental data were found to be dependent on temperature, strain rate and Z values according to the following expressions:

$$\begin{aligned} a &= 141.18\cdot(\ln(Z))^2 - 6301.6\cdot\ln(Z) + 69623 \\ b &= (-0.0099T + 1.5796)\cdot(\ln(\dot{\varepsilon}))^2 \\ &\quad + (-0.0977T + 14.844)\cdot\ln(\dot{\varepsilon}) + (-0.1966T - 2.0188) \end{aligned} \quad (6)$$

Model Predictions vs Experiments

Figure 9 shows a direct comparison between model-predicted and experimentally-obtained stress/strain curves for all the temperatures, at a selected strain rate of 0.01 s^{-1}. It is seen that the deviation between the two is reasonably small, which illustrates the suitability and validity of the proposed model for this particular wide range of conditions in HB-CD. Elimination of n and m values at elevated temperatures avoids the degradation in modeling accuracy at large plastic strain accumulations.

Another look at the results, for different strain rates at a given temperature, is provided in Figure 10. More deviation between experiments and predictions is noted, since the strain rate sensitivity of the material is stronger, however, the deviation is still quite reasonable and the model is capturing the varying trends of the stress/strain curves in response to changes in temperature, strain rates and strains. The model does particularly well at large strains (> 0.5) where a near steady state in the flow behavior is achieved. For 300 ºC in particular, the model shows the ability to capture the apparent hardening behavior associated with the higher strain rates, and the shift towards more of a softening behavior at lower strain rates.

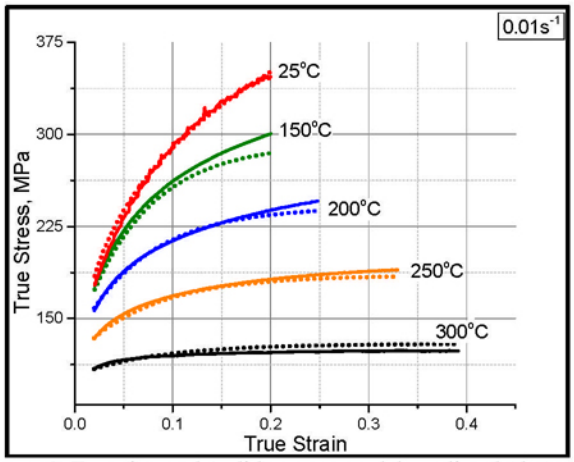

Figure 9: Experimental (solid) versus model-predicted (dot) true stress/strain curves for the entire temperature range of this work, at a selected strain rate of 0.01 s^{-1} (Note that the curves for 100 ºC coincide with 25 ºC, and thus were not shown here).

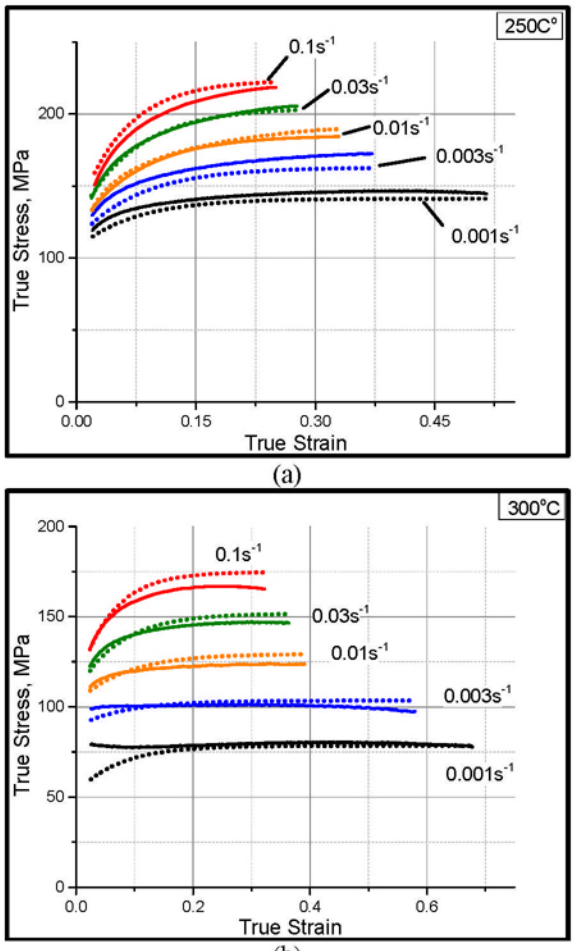

Figure 10: Experimental (solid) versus model-predicted (dot) true stress/strain curves for the entire strain rate range of this work, at a selected temperature of (a) 250 ºC and (b) 300 ºC.

Summary and Conclusions

HB-CD stamping has potentials for economic and fast forming of lightweight alloy sheets, such as aluminium, into automotive body panels. The deformation behavior of a selected material, AA5182-O, was studied in uniaxial tension at wide-raging temperatures (25-300 ºC) and strain rates (0.001-0.1 s^{-1}) that encompass the HB-CD process. Digital image correlation (DIC) was used to improve strain measurements and eliminate compliance issues. Results show that power-law breakdown is the dominant deformation mechanism at low/warm forming temperatures, with strong dynamic strain aging observed at or below 100 ºC. Strong shift in the deformation mechanism is noted at temperatures higher than 200 ºC, with clear evidence of dislocation climb at 300 ºC. A phenomenological constitutive model with a piece-wise function was developed and it was shown to successfully capture the evolving flow behavior of the material at different temperatures and strain rates, with a good match to experiments.

Acknowledgement

The authors are very grateful to the National Science Foundation (NSF) for supporting this work under grant # CMMI-1254670.

References

[1] W. Wen and J. G. Morris, "An investigation of serrated yielding in 5000 series aluminum alloys," *Materials Science and Engineering: A,* vol. 354, pp. 279-285, 2003.

[2] F. Ozturk, H. Pekel, and H. Halkaci, "The Effect of Strain-Rate Sensitivity on Formability of AA 5754-O at Cold and Warm Temperatures," *Journal of Materials Engineering and Performance,* vol. 20, pp. 77-81, 2011.

[3] R. C. Picu, "A mechanism for the negative strain-rate sensitivity of dilute solid solutions," *Acta Materialia,* vol. 52, pp. 3447-3458, 2004.

[4] P. Krajewski and J. Schroth, "Overview of Quick Plastic Forming Technilogy," *Materials Science Forum,* vol. 551-552, pp. 3-12, 2007.

[5] E. Taleff, P. Nevland, and P. Krajewski, "Tensile ductility of several commercial aluminum alloys at elevated temperatures," *Metallurgical and Materials Transactions A,* vol. 32, pp. 1119-1130, 2001.

[6] E. Taleff, G. Henshall, T. G. Nieh, D. Lesuer, and J. Wadsworth, "Warm-temperature tensile ductility in Al-Mg alloys," *Metallurgical and Materials Transactions A,* vol. 29, pp. 1081-1091, 1998.

[7] M.-A. Kulas, W. P. Green, E. Taleff, P. Krajewski, and T. McNelley, "Deformation mechanisms in superplastic AA5083 materials," *Metallurgical and Materials Transactions A,* vol. 36, pp. 1249-1261, 2005.

[8] F. Abu-Farha, "The development of a forming limit surface for 5083 aluminum alloy sheet," *JOM Journal of the Minerals, Metals and Materials Society,* vol. 63, pp. 72-78, 2011.

[9] D. Li and A. K. Ghosh, "Biaxial warm forming behavior of aluminum sheet alloys," *Journal of Materials Processing Technology,* vol. 145, pp. 281-293, 2004.

[10] N. Abedrabbo, F. Pourboghrat, and J. Carsley, "Forming of AA5182-O and AA5754-O at elevated temperatures using coupled thermo-mechanical finite element models," *International Journal of Plasticity,* vol. 23, pp. 841-875, 2007.

[11] R. Ayres and M. Wenner, "Strain and strain-rate hardening effects in punch stretching of 5182-0 aluminum at elevated temperatures," *Metallurgical Transactions A,* vol. 10, pp. 41-46, 1979.

[12] F. Abu-Farha and R. Curtis, "Quick-mount grips: Towards an improved standard for uniaxial tensile testing of metallic superplastic sheets," *Materialwissenschaft und Werkstofftechnik,* vol. 40, pp. 836-841, 2009.

[13] H. Halim, D. S. Wilkinson, and M. Niewczas, "The Portevin–Le Chatelier (PLC) effect and shear band formation in an AA5754 alloy," *Acta Materialia,* vol. 55, pp. 4151-4160, 2007.

[14] D. Thevenet, M. Mliha-Touati, and A. Zeghloul, "Characteristics of the propagating deformation bands associated with the Portevin–Le Chatelier effect in an Al–Zn–Mg–Cu alloy," *Materials Science and Engineering: A,* vol. 291, pp. 110-117, 2000.

[15] X. Feng, G. Fischer, R. Zielke, B. Svendsen, and W. Tillmann, "Investigation of PLC band nucleation in AA5754," *Materials Science and Engineering: A,* vol. 539, pp. 205-210, 2012.

[16] F. Kabirian, A. S. Khan, and A. Pandey, "Negative to positive strain rate sensitivity in 5xxx series aluminum alloys: Experiment and constitutive modeling," *International Journal of Plasticity,* vol. 55, pp. 232-246, 2014.

[17] J. G. Morris, "Dynamic strain aging in aluminum alloys," *Materials Science and Engineering,* vol. 13, pp. 101-108, 1974.

[18] W. A. Curtin, D. L. Olmsted, and L. G. Hector, Jr., "A predictive mechanism for dynamic strain ageing in aluminium-magnesium alloys," *Nat Mater,* vol. 5, pp. 875-80, Nov 2006.

[19] O. D. Sherby and P. M. Burke, "Mechanical behavior of crystalline solids at elevated temperature," *Progress in Materials Science,* vol. 13, pp. 323-390, 1968.

[20] E. M. Taleff and P. J. Nevland, "The high-temperature deformation and tensile ductility of Al alloys," *JOM,* vol. 51, pp. 34-36, 1999.

[21] H. J. McQueen and N. D. Ryan, "Constitutive analysis in hot working," *Materials Science and Engineering: A,* vol. 322, pp. 43-63, 2002.

[22] N. Abedrabbo, F. Pourboghrat, and J. Carsley, "Forming of aluminum alloys at elevated temperatures – Part 2: Numerical modeling and experimental verification," *International Journal of Plasticity,* 22, pp. 342-373, 2006.

[23] A. H. Boogaard van den, P. J. Bolt, and R. J. Werkhoven, "Aluminium sheet forming at elevated temperatures," in *International Conference on Numerical Methods in Industrial Forming Processes, NUMIFORM 2001*, ed. Toyohashi, Japan, 2001.

[24] H. S. Kim, M. Koç, and J. Ni, "Development of an analytical model for warm deep drawing of aluminum alloys," *Journal of Materials Processing Technology,* 197, pp. 393-407, 2008.

[25] Y. Q. Cheng, H. Zhang, Z. H. Chen, and K. F. Xian, "Flow stress equation of AZ31 magnesium alloy sheet during warm tensile deformation," *Journal of Materials Processing Technology,* vol. 208, pp. 29-34, 2008.

[26] Z. W. Xing, J. Bao, and Y. Y. Yang, "Numerical simulation of hot stamping of quenchable boron steel," *Fifth International Conference on Physical and Numerical Simulations of Material Processing, Zhengzhou, China, October 23-27, 2007.*